Development 130, 1493-1504

doi:10.1242/dev.00362

HASTY, the *Arabidopsis* ortholog of exportin 5/MSN5, regulates phase change and morphogenesis

Krista M. Bollman, Milo J. Aukerman, Mee-Yeon Park, Christine Hunter, Tanya Z. Berardini and R. Scott Poethig*

Department of Biology, University of Pennsylvania, Philadelphia, PA 19104-6018, USA
*Author for correspondence (e-mail: spoethig@sas.upenn.edu)

Accepted 23 December 2002

SUMMARY

Loss-of-function mutations of *HASTY* (*HST*) affect many different processes in *Arabidopsis* development. In addition to reducing the size of both roots and lateral organs of the shoot, *hst* mutations affect the size of the shoot apical meristem, accelerate vegetative phase change, delay floral induction under short days, adaxialize leaves and carpels, disrupt the phyllotaxis of the inflorescence, and reduce fertility. Double mutant analysis suggests that *HST* acts in parallel to *SQUINT* in the regulation of phase change and in parallel to *KANADI* in the regulation of leaf polarity. Positional cloning demonstrated that *HST* is the *Arabidopsis* ortholog of the importin β-like nucleocytoplasmic transport receptors *exportin 5* in mammals and MSN5 in yeast. Consistent with a potential role in nucleocytoplasmic transport, we found that HST interacts with RAN1 in a yeast two-hybrid assay and that a HST-GUS fusion protein is located at the periphery of the nucleus. HST is one of at least 17 members of the importin-β family in *Arabidopsis* and is the first member of this family shown to have an essential function in plants. The *hst* loss-of-function phenotype suggests that this protein regulates the nucleocytoplasmic transport of molecules involved in several different morphogenetic pathways, as well as molecules generally required for root and shoot growth.

Key words: nucleocytoplasmic transport, *Arabidopsis*, phase change, exportin

INTRODUCTION

The movement of macromolecules across the nuclear membrane is a central feature of the biology of eukaryotic cells. Nucleocytoplasmic transport is mediated by receptors (karyopherins) that bind cargo molecules and facilitate their transit through the nuclear pore (Chook and Blobel, 2001; Görlich and Kutay, 1999; Kaffman and O'Shea, 1999; Komeili and O'Shea, 2001; Macara, 2001; Nakielny and Dreyfuss, 1999). These nucleocytoplasmic transport receptors include proteins that regulate nuclear import (importins), proteins that regulate nuclear export (exportins), and proteins that import some proteins and export others. The macromolecules transported by various karyopherins have been defined primarily by biochemical methods in yeast and mammals, and often have conserved functions in these two organisms. These studies have shown that some karyopherins regulate the transport of a large number of functionally diverse proteins, whereas others have a more limited range of cargo molecules. Much less is known about the cellular and developmental processes for which these receptors are required, and how their activity is regulated by endogenous or environmental stimuli (Kaffman and O'Shea, 1999). In *Saccharomyces cerevisiae*, genetic analysis has revealed a requirement for specific karyopherins in both constitutive cellular processes and a variety of signal transduction pathways. Genetic evidence for the involvement of karyopherins in specific cellular and developmental processes in higher organisms is more limited, and thus far has been obtained for only three proteins in *Drosophila* (Lippai et al., 2000; Lorenzen et al., 2001; Tekotte et al., 2002; Tirian et al., 2000).

Nucleocytoplasmic transport operates by a similar mechanism in yeast and mammals (Chook and Blobel, 2001; Görlich and Kutay, 1999; Kaffman and O'Shea, 1999; Komeili and O'Shea, 2001; Macara, 2001). Karyopherins interact with cargo proteins at specific sites known as nuclear localization signals (NLS) or nuclear export sequences (NES). Most karyopherins bind directly to these sequences but a few bind via an adaptor protein, such as importin α, the adaptor for importin β. Nuclear transport is driven by the interaction between karyopherins and the small GTPase, Ran. Importins bind cargo molecules in the presence of Ran-GDP and release them upon binding Ran-GTP, whereas exportins bind cargo molecules in association with Ran-GTP and release them when Ran-GTP is hydrolyzed to Ran-GDP. Ran-GTP is kept at a relatively low level in the cytoplasm by the activity of the GTPase-activating protein RanGAP and the nucleotide-exchange factor RanBP1 (RCC), but is present at a relatively high level in the nucleus where these factors are absent. Importins bind cargo molecules in the cytoplasm, where Ran is primarily in its GDP-bound form, and release them in the nucleus, where the concentration of Ran-GTP is

relatively high. Conversely, exportins bind Ran-GTP and their cargo molecules in the nucleus, and dissociate from these molecules in the cytoplasm when Ran-GTP is hydrolyzed to Ran-GDP. Other factors that influence cargo binding include the phosphorylation state of the cargo and its association with factors that regulate the accessibility of the NLS or NES.

Although the mechanism of nuclear transport in plants has not been intensively studied, it is likely to be similar to the mechanism that has been described in other organisms (Merkle, 2001; Smith and Raikhel, 1999). Proper localization of proteins in plant cells depends on the same type of nuclear localization signal (Hicks and Raikhel, 1995) and nuclear export sequence (Haasen et al., 1999; Ward and Lazarowitz, 1999) that fulfill this function in other organisms. Furthermore, plants possess homologs of many of the proteins known to be involved in nucleocytoplasmic transport in other organisms. These include homologs of importin α (Ballas and Citovsky, 1997; Hubner et al., 1999; Jiang et al., 1998a; Jiang et al., 2001; Smith et al., 1997a; Smith et al., 1997b), importin β (Jiang et al., 1998a), the exportin Crm1/Xpo1 (Haasen et al., 1999), Ran1 (Haizel et al., 1997), RanGAP (Rose and Meier, 2001) and RanBP1 (Kim et al., 2001). Plant homologs of importin α (Hubner et al., 1999; Jiang et al., 1998a; Jiang et al., 2001) and importin β (Jiang et al., 1998b) have also been shown to mediate nuclear transport in animal cell systems, although with somewhat different properties than the homologous yeast and mammalian proteins.

The *HASTY* (*HST*) gene in *Arabidopsis* was originally identified in a screen for mutations that affect the transition between the juvenile and adult phases of vegetative development (Telfer and Poethig, 1998), and has also been identified in screens for mutations affecting leaf (Berna et al., 1999; Serrano-Cartagena et al., 2000) and floral (Berna et al., 1999; Eshed et al., 2001; Serrano-Cartagena et al., 2000) morphology. We present a detailed analysis of the *hst* phenotype that reveals a role for this gene in many different aspects of plant development. The basis for this pleiotropic phenotype is suggested by the discovery that *HST* encodes a protein similar to the karyopherins exportin 5 (Xpo5) in mammals and Msn5p in yeast (Alepuz et al., 1999; Bohnsack et al., 2002; Brownawell and Macara, 2002; Calado et al., 2002; Görlich et al., 1997; Kaffman et al., 1998). The *hst* loss-of-function phenotype indicates some of the developmental pathways for which HST is required, and suggests that regulation of nucleocytoplasmic transport may play an important role in these pathways.

MATERIALS AND METHODS

Growth conditions

All of the genetic stocks described in this paper are in a Columbia (Col) genetic background. Analyses of leaf and inflorescence morphology were conducted using plants grown in pots in Metromix 200 (Scotts). Seedling growth and morphology was studied using plants grown vertically in petri dishes on a medium consisting of 1/2× MS salts (Gibco BRL), 0.5 g/l MES, 5% sucrose, 0.8% agar (pH 5.7). Seeds were stratified at 4°C for 2-3 days before being transferred to a growth chamber, and were grown at 22°C under continuous fluorescent illumination unless otherwise noted.

Phenotypic analysis

Abaxial trichomes were scored by observing seedlings 10-18 days after planting with a stereomicroscope. Leaf morphology was recorded by photocopying leaves attached to cardboard with double-sided tape. These photocopies were subsequently scanned into a computer and manipulated with Photoshop to produce the images presented here. The rate of leaf initiation was measured using plants homozygous for a *LFY::GUS* transgene obtained from D. Weigel (Salk Institute). Soil-grown plants were harvested on successive days and stained for GUS activity, and the number of leaf primordia was then counted with the aid of a compound microscope.

GUS activity was observed by incubating seedlings overnight in 1 mM X-gluc, 50 mM sodium phosphate buffer (pH 7), 0.5 mM potassium ferricyanide, 0.5 mM potassium ferrocyanide and 0.1% Triton X-100 at 37°C followed by decolorization in 95% ethanol. They were then dehydrated in 100% ethanol, transferred to xylene and mounted in Permount on microscope slides. Specimens expressing *35S::LFY* were stained overnight; specimens expressing *35S::HST-GUS* were stained for 2 hours.

Histology

Seedlings were fixed overnight at 4°C in 3% glutaraldehyde in 0.5 M phosphate buffer (pH 5.7), post-fixed in 1% OsO_4 for 2 hours, and then dehydrated and embedded in Spurr's resin. Sections were stained with 1% Methylene Blue in 1% sodium borate. Scanning electron microscopy was performed on flowers fixed in FAA (Jensen, 1962).

Positional cloning

F_2 progeny of a cross between *hst-1* (Col) and wild-type Landsberg erecta (L*er*) were screened for kanamycin resistance either by spraying soil-grown plants with 200 μg/ml kanamycin one week after planting, or by sowing F_2 seeds on germination medium containing 50 μg/ml kanamycin. Kanamycin-resistant plants that were homozygous *hst-1* were allowed to set self seed at 18°C. RFLP polymorphisms were scored using DNA isolated from 10 or more progeny of these recombinant F_2 plants. RLFPs useful for mapping *hst-1*, as well as allele-specific RFLPs associated with *hst* mutations, were identified by hybridizing radioactively labeled BAC clones to blots of genomic DNA digested with a variety of restriction enzymes.

HST cDNAs were isolated using standard methods (Sambrook et al., 1989) from size-fractionated cDNA libraries (Kieber et al., 1993) obtained from the Arabidopsis Biological Resource Center. Bluescript plasmids (pBS SK–) were excised from lambda clones using a rapid excision kit (Stratagene) and the protocol supplied by the manufacturer.

Northern analysis

RNA for northern analysis was prepared from leaf and floral bud tissues from mature plants, and from root tissue from plants grown in culture. RNA was prepared using TRIzol reagent (GibcoBRL) and poly(A) RNA was isolated using the Oligotex mRNA kit (Qiagen). PolyA RNA (0.75 μg) was run on a 1.2% agarose gel containing 3% formaldehyde and then transferred to Hybond N^+ membrane (Amersham). Hybridization was carried out according to Sambrook et al. (Sambrook et al., 1989), using a 0.7 kb 5′ fragment of the *HST* cDNA.

Transgenes

The *HST* cDNA (AY198396) was placed under the regulation of the CaMV 35S promoter in pCAMBIA 3301. The *HST*-coding region was amplified from a cloned *HST* cDNA template using primers 5′-GCGGATCCATGGAAGATAGCAACTCCACG-3′ and 5′-CGGATCCGCTAGCTCATTGTACGAACTCTTCATCC-3′ that included the start and stop codons, respectively. The 5′ primer also included an *Nco*I site, and subsequent digestion of the PCR product with *Nco*I generated a *HST* cDNA with an *Nco*I end and a blunt end. pCAMBIA 3301 was digested with *Bst*EII to remove the β-

Table 1. Vegetative phase change in *hst*, wild-type and *35S::HST* plants

Photoperiod	Genotype	Juvenile leaves*	Transition leaves†	Adult leaves‡	Total leaves	Bracts	First open flower (DAP§)	*n*
Continuous light	Wild type	3.8±0.1	2.2±0.1	4.6±0.3	10.6±0.3	2.2±0.1	20.1±0.2	24
Continuous light	*hst-1*	1.7±0.1	0.3±0.0	3.7±0.2	5.7±0.2	1.9±0.1	19.5±0.2	23
Continuous light	*hst-6*	1.8±0.1	0.2±0.0	3.4±0.2	5.4±0.2	1.7±0.1	19.1±0.2	33
Continuous light	*hst-1; 35S::HST*	4.0±0.1	2.1±0.2	4.3±0.1	10.4±0.1	2.1±0.1	20.9±0.2	20
Continuous light	*hst-1; 35S::HST-GUS*	4.2±0.1	2.2±0.2	4.5±0.2	10.9±0.2	3.0±0.1	n.d.	15
Long days	Wild type	4.5±0.1	2.8±0.1	3.7±0.2	11.1±0.1	3.0±0.1	26.8±0.2	17
Long days	*hst-1*	2.0±0.0	0	3.3±0.3	5.3±0.2	2.6±0.1	26.4±0.2	23
Short days	Wild type	7.3±0.6	n.d.	39.2±1.6	46.5±2.0	10.3±0.5	70.1±0.5	12
Short days	*hst-1*	2.8±0.2	n.d.	69.5±2.9	71.3±2.8	16.6±0.8	95.0±0.5	14

*Leaves without abaxial trichomes.
†Leaves partially covered with abaxial trichomes.
‡Leaves completely covered with abaxial trichomes.
§Days after planting.
Values are ±s.e.m.
n.d., not determined.

glucuronidase gene, blunt-ended with Klenow enzyme and digested with *Nco*I. The vector fragment was gel-purified and ligated to the *HST* cDNA to generate the HST over-expression construct. A *HST-GUS* fusion construct was generated by amplifying the *HST*-coding region minus the stop codon from the *HST* cDNA using primers 5′-GCGGATCCATGGAAGATAGCAACTCCACG-3′ and 5′-GCGGATCCATGGATTGTACGAACTCTTCATCC-3′, which added *Nco*I sites at each end of the amplicon. *Nco*I-cut PCR product was then inserted into the *Nco*I site of vector pCAMBIA 3301, to generate a translational fusion between the 3′ end of the *HST* gene and the 5′ end of the *Escherichia coli uidA* gene encoding β-glucuronidase. Both constructs were used to transform wild-type (Col) and *hst-1* (Col) plants using the floral dip method (Clough and Bent, 1998), and transformants were selected by spraying the seedlings produced by these plants with 250 mg/l glufosinate (AgrEvo).

Two-hybrid interaction between RAN1 and HST

The coding region of *Arabidopsis RAN1* (Haizel et al., 1997) was amplified from first-strand cDNA products generated by reverse transcription of RNA isolated from *Arabidopsis* seedlings. The RT-PCR reaction employed a 5′ *RAN*-specific primer with an *Eco*RI site, (5′-GGAATTCATGGCTCTACCTAACCAGCAAACCG-3′) and a 3′ *RAN*-specific primer with a *Bam*HI site (5′-CGGATCCTTAC-TCAAAGATATCATCATCGTC-3′). Upon digestion with *Eco*RI and *Bam*HI, the PCR product was inserted into *Eco*RI/*Bam*HI-digested pGBKT7 (Clontech) to generate the *RAN1*:BD vector. To generate the *HST*:BD vector, the *HST*-coding region was amplified from the *HST* cDNA using primers flanked by *Nco*I sites, and was inserted into *Nco*I-digested pGADT7. The ΔN-*hst*:AD vector, which contains an 106 N-terminal deletion of *HST*, was created in a similar fashion using the primers 5′-AGACCATGGCTCTTAAGAGTCAGTCTGCT-3′ and 5′-GCGGATCCATGGATTGTACGAACTCTTCATCC-3′. The *hst-3*:AD vector was created by in vitro mutagenesis (Stratagene Quick Change kit) of the *HST*-AD vector to introduce a mutation present in *hst-3*. Yeast transformation and subsequent two-hybrid analyses were carried out according to the Matchmaker protocol (Clontech). In addition, we made constructs to test the reciprocal two-hybrid interaction, i.e. *RAN* fused to pGADT7 and *HST* fused to pGBKT7, but we were unable to recover *RAN-GAD* transformants, which suggests that this construct somehow affected yeast growth.

RESULTS

All of the results presented in this paper were obtained using *hst-1*. Because the phenotype of *hst-1* is identical to a likely null allele, *hst-6* (Table 1), we believe the phenotype of *hst-1* represents the null phenotype of this gene. Previous studies have described several of the effects of *hst-1* on plant morphology. These include: a reduction in the size of leaves, sepals and petals; up-rolling of the leaf blade; a reduction in leaf number; accelerated production of abaxial trichomes; disrupted phyllotaxis in the inflorescence; and reduced male and female fertility (Fig. 1) (Serrano-Cartagena et al., 2000; Telfer and Poethig, 1998). *hst* mutations have also been reported to enhance the floral phenotype of *kan; pkl* double mutants (Eshed et al., 2001). We confirmed and extended these observations, and found that this phenotype can be attributed to defects in several different processes, including cell growth, phase change and the specification of organ polarity.

Seedling development

hst-1 has significant effects on root and hypocotyl development under both dark and light conditions. *hst-1* seedlings grown in the dark, on a medium containing 5% sucrose, have an open apical hook and irregularly oriented cotyledons; wild-type seedlings typically have a tight apical hook and appressed cotyledons (Fig. 2A). Light- or dark-grown *hst-1* seedlings also have an abnormally short hypocotyl and primary root (Fig. 2A,B,I). The effect of *hst-1* on root length is attributable to both a decrease in the rate of root elongation and premature cessation of root growth (Fig. 2I). *hst-1* roots grow at a rate of about 0.9 mm/day, compared with 2.6 mm/day for wild type, and cease elongating by 9 days after planting. This defect in root growth is accompanied by the production of adventitious roots from the base of the hypocotyl (Fig. 2B). *hst-1* has no obvious effect on the anatomy of the hypocotyl and root (Fig. 2G,H), which suggests that its effect on root and hypocotyl growth does not result from a change in cell identity, as is the case for several other mutations that produce short roots (Benfey et al., 1993). However, *hst-1* does affect the anatomy of the shoot apical meristem (SAM): 3-day-old *hst-1* seedlings (Fig. 2F) have a larger and more rounded SAM than do wild-type seedlings (Fig. 2C). The primordia of leaves 1 and 2 are also smaller than normal in 3-day-old *hst-1* seedlings (Fig. 2F), probably because their initiation is delayed relative to wild type (see below).

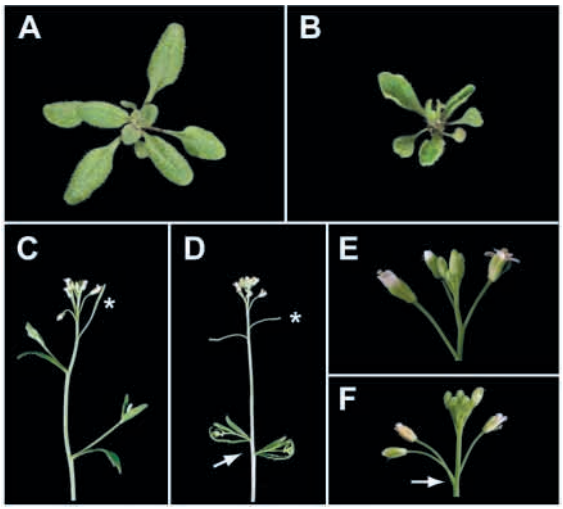

Fig. 1. The phenotype of *hst-1*. (A) Two-week-old wild-type rosette (B) Two-week-old *hst-1* rosette. (C) Wild-type inflorescence. (D) *hst-1* inflorescence. Note abnormally expanded internodes and short lateral inflorescences (arrow) and unfertilized siliques (asterisk). (E) Wild-type flowers. (F) *hst-1* flowers. *hst-1* flowers are unusually small and are irregularly spaced (arrow).

Vegetative phase change

The juvenile and adult phases of vegetative development in *Arabidopsis* are distinguishable by differences in leaf size and shape and by the distribution of trichomes on the leaf blade (Chien and Sussex, 1996; Röbbelen, 1957; Steynen et al., 2001; Telfer et al., 1997; Telfer and Poethig, 1994; Tsukaya et al., 2000). The first four rosette leaves of wild-type plants (juvenile leaves) are round or elliptical, have a smooth margin, a low ratio of blade length to petiole length, lack trichomes on their abaxial surface and have a relatively low density of trichomes on their adaxial surface (Fig. 3; Table 1). The adult phase starts with the production of leaf 5 or 6, and is marked by the production of more highly serrated leaves that have a high blade:petiole ratio and an increased capacity for trichome production on both their abaxial and adaxial surfaces. Between these two phases there is a brief transition phase, which is defined by the production of leaves that are partially covered with abaxial trichomes.

In *hst-1*, the onset of abaxial trichome production (Fig. 3A; Table 1), the increase adaxial trichome density (Fig. 3B) and the decline in blade:petiole ratio (Fig. 3C) begin with leaf 3 and proceed unusually quickly after this point. To determine if this phenotype reflects a change in timing of the juvenile-to-adult transition, we examined the effect of *hst-1* on the rate of leaf and floral initiation (Fig. 3D). For this purpose, we took advantage of plants carrying the *LFY::GUS* transgene because this gene makes it possible to observe leaf and floral bud primordia at an early stage in their development (Blazquez et al., 1997). Under continuous light (CL), *hst-1* seedlings exhibited a slight delay in leaf initiation during germination but went on to produce leaves at the same rate as wild type throughout the rest of vegetative development. *hst-1* plants produced their first leaf with abaxial trichomes (leaf 2.6±0.1) 3.8 days after planting (DAP), whereas wild-type plants produced this leaf (leaf 4.8±0.1) 2 days later. Mutant plants

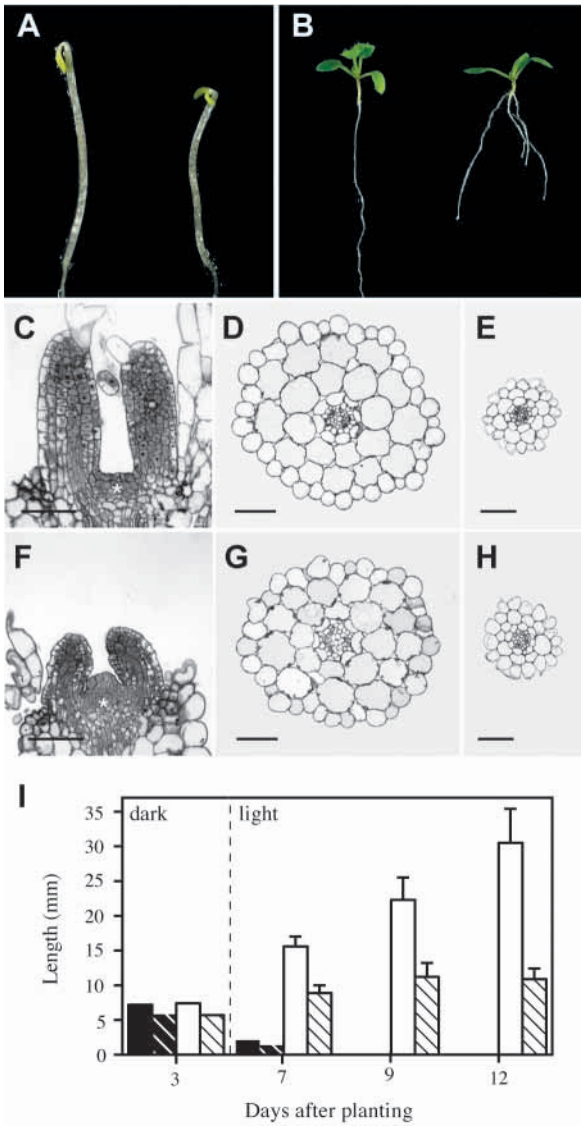

Fig. 2. The effect of *hst* on seedling morphology. (A) Three-day-old wild-type (left) and *hst-1* (right) seedlings grown in the dark. (B) Seven-day-old wild-type (left) and *hst-1* (right) seedlings grown in the light. (C-E) Anatomy of 3-day-old wild-type seedlings. (F-H) Anatomy of 3-day-old *hst-1* seedlings. (C,F) Median longitudinal section of the shoot apex; the meristem is marked with an asterisk. (D,G) Cross-section of the hypocotyl. (E,H) Cross-section of the root. (I) Length of the hypocotyl and root in dark- and light-grown seedlings. Black, wild-type hypocotyl; white, wild-type root; white hatching on black, *hst-1* hypocotyl; black hatching on white, *hst-1* root. Scale bars: 50 μm.

also initiated floral buds 2 days earlier than did wild type. Thus, *hst-1* accelerates both the juvenile-to-adult transition and floral induction. The early flowering phenotype of *hst-1* is completely attributable to its effect on vegetative phase change because flower initiation occurred 7 days after the juvenile-to-adult transition in both mutant and wild-type plants.

Although *hst-1* accelerates floral induction, it has a more variable effect on bolting and the appearance of the first open flower. *hst-1* plants sometimes bolt and produce mature flowers earlier than normal (Table 1), but may flower later than

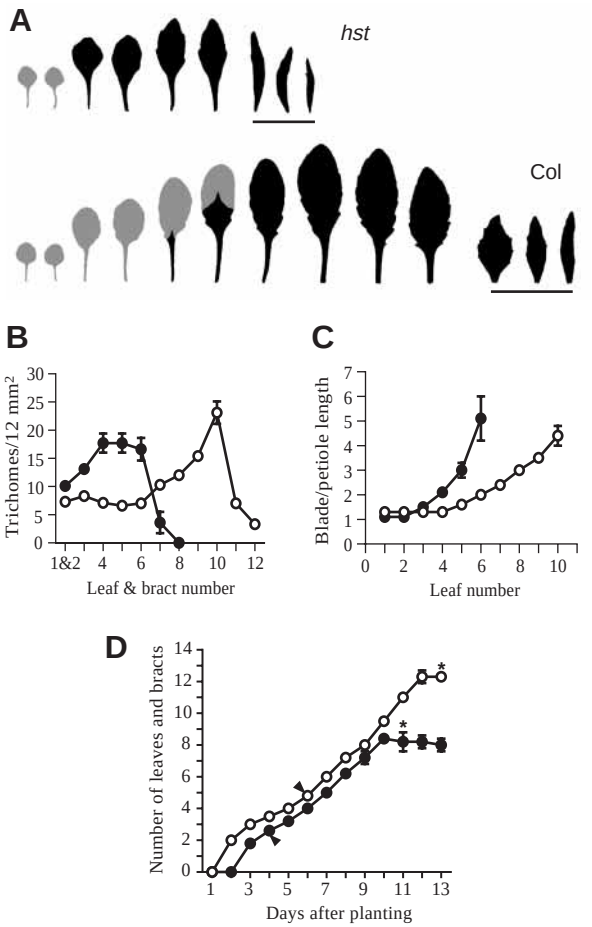

Fig. 3. Effect of *hst-1* on phase change. (A) Rosette leaf and bract morphology of *hst-1* and wild-type plants (Col). Gray, no abaxial trichomes; black, abaxial trichomes; underline, bracts. (B) Adaxial trichome density of rosette leaves and bracts in *hst-1* and wild-type plants (C) The blade:petiole length ratio of rosette leaves in *hst-1* and wild-type plants. (D) Rate of leaf initiation in *hst-1* and wild-type plants. Arrows indicate the position of the first leaf with abaxial trichomes in siblings of the dissected plants; asterisks indicate the time at which GUS-stained floral buds were visible. White circles, wild type; black circles, *hst-1*.

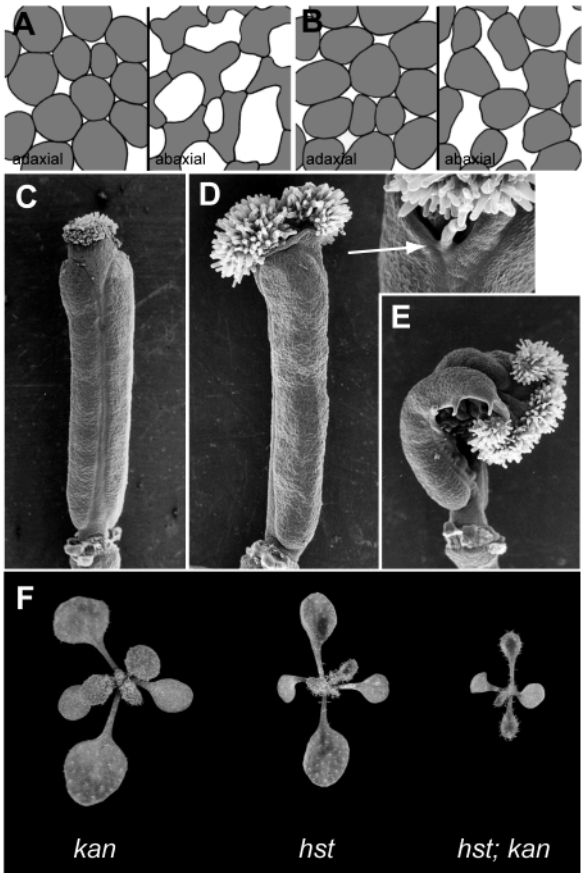

Fig. 4. Effect of *hst-1* on leaf and carpel polarity. (A,B) Paradermal views of the adaxial and abaxial mesophyll layers of leaf 3 from wild-type (A) and *hst-1* (B) plants. (C-E) Scanning electron micrographs of wild-type (C) and *hst-1* (D,E) pistils; note the ovules located along the margins of the carpels (arrow). (F) Phenotype of *kan-11*, *hst-1* and *hst-1; kan-11* seedlings. Double mutant seedlings have more severely up-rolled leaves and cotyledons, and have a significantly larger number of abaxial trichomes than either single mutant.

wild-type plants under some conditions. For example, the *hst-1* plants illustrated in Fig. 3D produced their first open flower 1 day later than normal (24.3 DAP versus 23.5 DAP) even though they produced floral buds 2 days early. This observation suggests that bolting and floral maturation are either regulated independently of floral initiation in mutant plants, or that *hst-1* delays bolting and floral maturation after floral initiation has taken place. Given the effect of *hst-1* on root and hypocotyl growth, we believe that the latter explanation is more likely.

Unexpectedly, *hst-1* has opposite effects on flowering time in short days (SD). Although mutant plants flower slightly earlier than normal in long days (LD; 16 hours light:8 hours dark) or continuous light, they flower much later and with nearly twice as many leaves and bracts as wild-type plants in SD (8 hours light:16 hours dark) (Table 1). We conclude HST normally acts to repress flowering in LD and to promote flowering in SD.

Organ polarity

The first two leaves of *hst-1* plants are generally flat or only slightly up-rolled, but subsequent leaves curve strongly upward (Fig. 1B). This effect on leaf expansion is associated with a loss of tissue polarity within the mesophyll of the leaf blade. In wild-type leaves, cells in the upper mesophyll are spherical or slightly cylindrical in shape and are densely packed, whereas cells in the lower mesophyll layer are irregular in shape and are separated by large air spaces (Fig. 4A). Although the upper mesophyll layer of *hst-1* appears normal, cells in the lower spongy layer are more regular in shape and have less intercellular space than normal (Fig. 4B), which causes this layer to resemble the upper (adaxial) mesophyll layer. A role for HST in the regulation of organ polarity is also apparent in the effect of *hst-1* on carpel development. Although the carpels of *hst-1* flowers are quite normal early in the growth of the inflorescence, older inflorescences typically produce flowers with a laterally expanded stigma, unfused carpels and external ovules (Fig. 4D,E). The severity of this defect varies between plants, but occurs in ~30% of flowers (n=277). The defect in

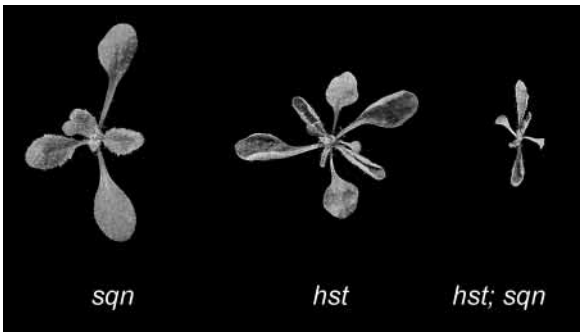

Fig. 5. The genetic interaction between *hst-1* and *sqn-1*. Double mutants are smaller and produce many more abaxial trichomes on leaves 1 and 2 than single-mutant plants.

carpel fusion and ovule production is usually limited to the apical end of the carpels although, in rare cases, it may extend along their entire length (Fig. 4E). This phenotype is characteristic of adaxializing mutations, e.g. mutations in members of the *YABBY* (Bowman, 2000; Siegfried et al., 1999) and *KANADI* (*KAN*) (Eshed et al., 2001; Kerstetter et al., 2001) gene families, and suggests that HST may regulate abaxial polarity in carpels as well as in leaves.

The interaction between *hst-1* and the adaxializing mutation *kan-11* (Kerstetter et al., 2001) is consistent with the hypothesis that HST regulates adaxial/abaxial polarity. We found that *hst-1; kan-11* double mutants had more highly up-rolled cotyledons and leaves (Fig. 4F) and produced significantly more abaxial trichomes on leaves 1 and 2 than did either single mutant. In a 16 mm^2 area of leaf 1 or 2, *kan-11* had an average of 2.2±0.4 abaxial trichomes and 10.3±0.5 adaxial trichomes, *hst-1* had 0.3±0.1 abaxial and 12.5±0.7 adaxial trichomes, and *hst-1; kan-11* seedlings had an average of 11.9±8 abaxial and 11±0.5 adaxial trichomes. Because *hst-1; kan-11* seedlings did not exhibit an increase in adaxial trichome density (and, in fact, had equal numbers of trichomes on both surfaces of the leaf), we attribute the synergistic effect of these mutations on abaxial trichome production to a loss of leaf polarity, rather than to an overall increase in the capacity for trichome production.

HST interacts with SQUINT

Mutations in *SQUINT* (*SQN*), the *Arabidopsis* ortholog of cyclophilin 40, are phenotypically similar to *hst* mutations in that they slightly delay leaf initiation (albeit at a different stage in shoot development), accelerate vegetative phase change and produce aberrant phyllotaxy in the inflorescence as well as abnormal patterns of carpel development (Berardini et al., 2001). To determine the genetic relationship between these two genes, we examined the phenotype of *hst-1, sqn-1* plants. Double mutant seedlings had a much more severe phenotype than either single mutant (Fig. 5). In addition to being significantly smaller than both *sqn-1* and *hst-1*, double mutants produced large numbers of abaxial trichomes starting with leaf 1. By contrast, *hst-1* and *sqn-1* did not produce abaxial trichomes until leaf 3, and had only a few abaxial trichomes on this leaf. We conclude that *SQN* and *HST* either operate cooperatively in the same regulatory pathway or operate in parallel pathways.

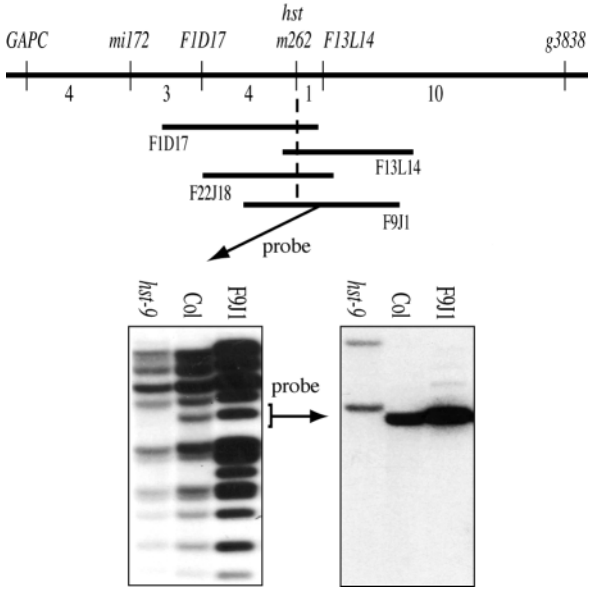

Fig. 6. Positional cloning of *HST*. The top line indicates the genetic map of the region surrounding *hst-1*, as determined from an analysis of F_2 progeny from a cross to L*er*. The number of recombinants in each interval is indicated below the line. BACs that hybridized to the lamba clone *m262*, which showed no recombination with *hst-1*, are shown below this line. Hybridization of F9J1 to an *Eco*RV digest of genomic DNA from *hst-9* and Col revealed a missing fragment in *hst-9*. When this *Eco*RV fragment was gel purified from F9L1 DNA and used to re-probe the blot, it hybridized to two fragments in *hst-9*. These fragments are not visible in the blot hybridized with the entire BAC because this blot was under-exposed in order to visualize as many fragments as possible.

Cloning HST

hst-1 maps to chromosome 3, ~0.8 cM south of *GAPC* (Telfer and Poethig, 1998). Recombinants between *GAPC* and *hst-1* were isolated by screening 650 F_2-*hst* plants from a cross of *hst-1* (Col) to L*er*. Recombinants to the south of *hst-1* were identified by screening for kanamycin-resistant *hst* plants in F_2 families from a cross of *hst-1* to DsTn 108, an L*er* line containing a kanamycin-resistant transgene located 3 cM south of *GAPC* (Bancroft and Dean, 1993). Existing RFLP markers from this region were mapped relative to *hst-1* using this collection of recombinant lines. The most tightly linked marker, lambda clone *m262*, detected an *Xho*1 polymorphism that was not recombinant in any of these lines (Fig. 6). *m262* was hybridized to the IGF bacterial artificial clone (BAC) library to identify larger clones from this region. Two such clones, F1D17 and F13L14, identified *Eco*RV and *Hin*dIII RFLPs on either side of *hst-1*, demonstrating that these BACs span the *HST* locus. These and other overlapping BACs were then hybridized to Southern blots of DNA from all existing *hst* mutant alleles in order to identify allele-specific polymorphisms. The clone F9J1 revealed a 5.5 kb *Eco*RV band that was present in wild-type Col plants but absent in *hst-9* (Fig. 6). This 5.5 kb fragment hybridized to two restriction fragments in *Eco*RV digests of *hst-9* DNA, which implies that the mutation in *hst-9* is located in this fragment and is likely to be an inversion (Fig. 6). Hybridization of this *Eco*RV fragment to a seedling cDNA library produced cDNAs corresponding to a single gene. The

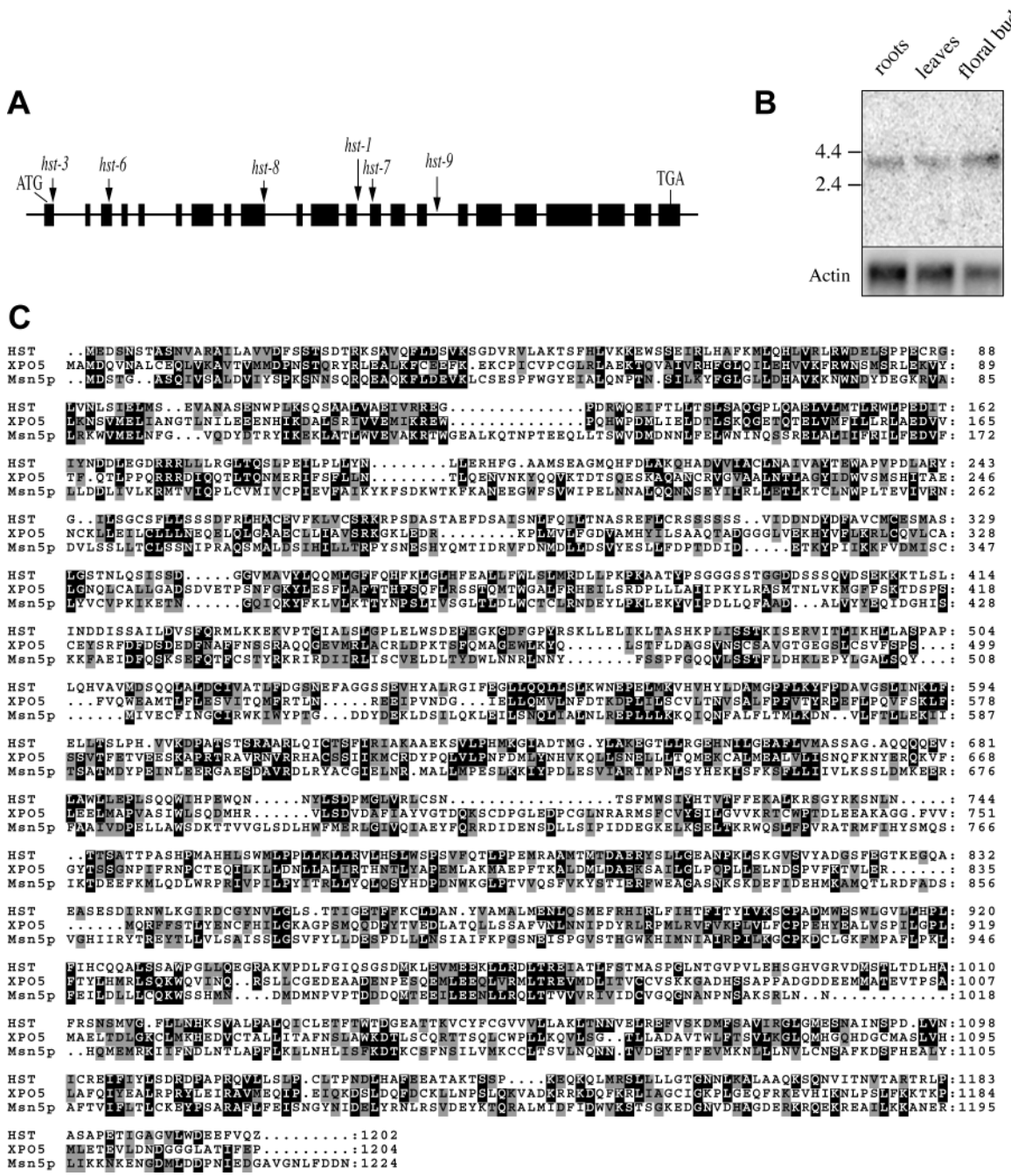

Fig. 7. Molecular characterization of *HST*. (A) Genomic structure. Exons are indicated by boxes. Arrows indicate the position of mutations described in the text. (B) Poly(A)-enriched RNA from leaves, roots and floral buds hybridized with a 5′ fragment of the *HST* cDNA. This blot was stripped and re-hybridized with an actin probe, which served as a loading control. (C) CLUSTAL X 1.81 alignment of the amino acid sequence of HST (AY198396), human Xpo5 (NP_065801) and Msn5p (NP_010622) from *S. cerevisiae*. Amino acids identical in two or more sequences are highlighted in black; similar amino acids are highlighted in gray.

longest of these cDNAs (AY198396) is 3840 bp, consists of 22 exons and encodes a protein of 1202 amino acids with a predicted molecular weight of 133 kDa (Fig. 7A). Hybridization of this cDNA to poly(A)-enriched RNA revealed a single 4 kb transcript in leaves, roots and floral buds (Fig. 7B), an expression pattern that is consistent with the fact that *HST* has a mutant phenotype in all of these organs.

All of the *hst* alelles we analyzed had mutations in the predicted *HST* transcript (Fig. 7A). *hst-1* is a single base transversion that changes the conserved GT to GA at the splice donor site of the 12th intron. RT-PCR reactions with primers that flank this intron demonstrated that it is not spliced from pre-mRNA in *hst-1* (data not shown), resulting in an in-frame stop codon 31 bp after the exon-intron junction. *hst-3* is a 3 bp deletion in exon 1 that replaces amino acids $D^{36}S^{37}$ with an A. *hst-6* contains a G to A transition that results in a stop codon

at position 107 in the predicted protein. This fragment represents only 9% of the full-length protein, which suggests that *hst-6* is likely to be a null allele. *hst-7*, an X-ray-induced allele, has a 7 bp deletion in exon 13 that introduces a stop codon in the open reading frame 12 bp after this mutation. *hst-8* has a 24 bp in-frame deletion in exon 9. *hst-9* is a 300 kb inversion with breakpoints in intron 15 and in the last exon of At3g05770, a transcribed gene of unknown function.

To determine the effect of overexpressing *HST*, the *HST* cDNA was fused to the CaMV 35S promoter in pCAMBIA 3301 and the resulting construct was introduced into *hst-1* plants by Agrobacterium transformation. This transgene was capable of completely rescuing the mutant phenotype of *hst-1* (Table 1), demonstrating that it encodes a functional HST protein. Wild-type plants transformed with this construct, and which expressed high levels of HST mRNA (data not shown), were completely normal. In order to ensure that the absence of phenotypically aberrant plants was not due to loss-of-function mutations in the transgene, an insertion that completely rescued the *hst*-mutant phenotype (Table 1) was crossed into a Col genetic background. Col plants carrying a single copy of this transgene were not obviously different from their wild-type siblings: transgenic plants (n=13) had 4.6±0.2 juvenile leaves and 5.5±0.3 adult leaves, whereas their wild-type siblings (n=29) had 4.4±0.1 juvenile leaves and 5.5±0.2 adult leaves. This result suggests either that plants are insensitive to levels of the HST protein above the wild-type amount, or that *HST* is post-transcriptionally regulated.

HST is similar to exportin 5

HST encodes a protein consisting of 1202 amino acids (133 kDa) with approximately 12 regions that have similarity to the HEAT repeats typically found in karyopherins in the importin β family (http://www.embl-heidelberg.de/~andrade/papers/rep/search.html) (Andrade et al., 2001). BLAST searches of non-redundant databases at GenBank revealed that HST is similar in both size and amino acid sequence to the mammalian karyopherin exportin 5 (Xpo5) (1204 amino acids, 136 kDa) and the orthologous protein Msn5p (1224 amino acids, 142 kDa) from *Saccharomyces cerevisiae* (Fig. 7C). *Arabidopsis* genes encoding importin β-like proteins were identified by searching the *Arabidopsis* genome database (http://arabidopsis.org/wublast/index2.html) for proteins with similarity to members of this family in yeast and mammals. *Arabidopsis* has at least 17 predicted members of the importin β family. These *Arabidopsis* proteins are much more similar to mammalian proteins than to their yeast homologs. A cladogram illustrating the relationship between human importin β-like proteins and predicted members of this family in *Arabidopsis* is shown in Fig. 8. HST is the most closely related protein in *Arabidopsis* to Xpo5 and Msn5p, and is more similar to Xpo5 than it is to any other protein in *Arabidopsis*. We conclude that *HST* is the *Arabidopsis* ortholog of *Xpo5/MSN5*.

HST interacts with RAN1

Like many other karyopherins (Görlich and Kutay, 1999; Komeili and O'Shea, 2001; Macara, 2001; Nakielny and Dreyfuss, 1999), the interaction between Xpo5/Msn5p their cargo molecules is regulated by Ran (Brownawell and Macara, 2002; Bohnsack et al., 2002; Calado et al., 2002). To test if

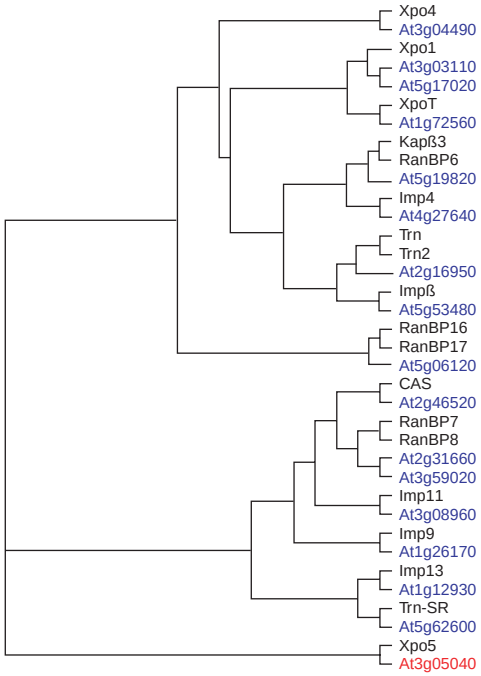

Fig. 8. Unrooted bootstrap (1000 reiterations) cladogram of human and *Arabidopsis* importin β-like proteins. This tree was generated by neighbor-joining using Clustal X 1.81 and was visualized using TreeView. Black, human; blue, *Arabidopsis*; red, HST. Accession Numbers for human proteins: CAS (NP_001307), KAPβ3 (NP_002262), IMPβ (NP_002256), IMP4 (NP_078934), IMP9 (NP_060555), IMP11 (NP_057422), IMP13 (NP_055467), RANBP6 (AAC14260), RANBP7 (NP_006382), RANBP8 (NP_006381), RANBP16 (NP_055839), RANBP17 (NP_075048), TRN (NP_002261), TRN2 (NP_038461), TRNSR (NP_036602), XPO1 (NP_003391), XPO4 (BAB21812), XPO5 (NP_065801), XPOT (NP_009166). Sequences of *Arabidopsis* proteins are available at www.tigr.org/tdb/e2k1/ath1/LocusNameSearch.shtml.

HST interacts with Ran we took advantage of the yeast two-hybrid assay. For this purpose, the coding region of *Arabidopsis RAN1* was fused to the DNA-binding domain of *GAL4* in the plasmid pGBKT7 to produce *RAN1*:AD, and the *HST* coding region was fused to the *GAL4* activation domain in pGADT7 to produce *HST*:BD. As negative controls, we produced a construct containing a 106 amino acid N-terminal deletion of *HST*, encompassing the putative Ran-binding domain (ΔN-*hst*:BD), and a construct containing the *hst-3* mutation (*hst-3*:BD), which lies in this region. Cells containing the *HST*:BD and *RAN1*:AD constructs grew under stringent conditions, whereas strains containing either *hst-3*:BD or ΔN-*hst*:BD and *RAN1*:AD grew very poorly (Fig. 9). This result is consistent with the results of a similar experiment performed with Xpo5 (Brownawell and Macara, 2002), and suggests that HST has Ran-binding activity.

HST is located at the periphery of the nucleus

To determine the subcellular distribution of HST, we produced transgenic *Arabidopsis* plants expressing a HST-GUS fusion protein under the regulation of the CaMV 35S promoter. *hst-1* plants containing the transgene were phenotypically wild type (Table 1), demonstrating that the fusion protein was functional.

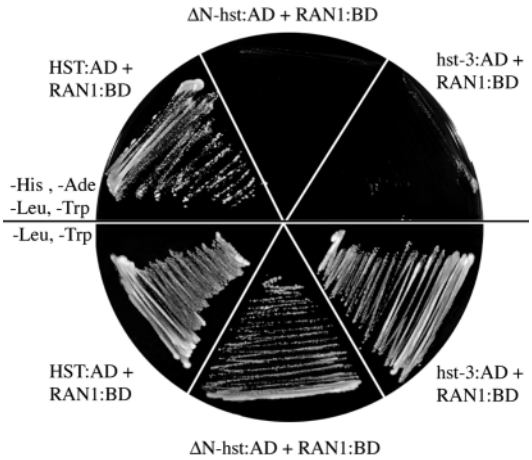

Fig. 9. Two hybrid analysis of the interaction between HST and RAN1. Cells transformed simultaneously with the indicated vectors were selected for the presence of both constructs on medium lacking Leu and Trp, and then plated on a medium lacking Leu, Trp, His and Ade to test for the interaction between the AD and BD constructs. Cells containing the *HST*:BD and *RAN1*:AD vectors grew on this restrictive medium and expressed β galactosidase (not shown). Cells containing *RAN1*:AD and either the *hst-3*:BD or ΔN-*HST*:BD vectors grew very poorly or not at all on this medium, and did not express β galactosidase.

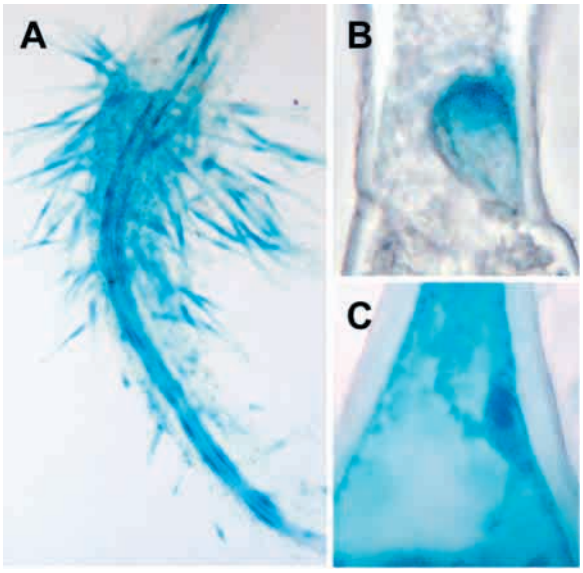

Fig. 10. Location of GUS activity in *hst-1* plants homozygous for a *35S::HST-GUS* transgene. (A) Seedling root, (B) trichome and (C) trichome of a plant transformed with the *35S::GUS* vector used in the production of the *35S::HST-GUS* fusion construct.

GUS activity was concentrated in the nucleus and the surrounding cytoplasm in root hairs and trichomes, and in cells in the stele and stipules (Fig. 10). In trichomes, which are large cells with large polyploid nuclei, GUS staining was clearly localized in the vicinity of the nuclear membrane and was always most intense on the apical side of the nucleus (Fig. 10B). This is in contrast to the widespread distribution of GUS activity in cells transformed with a control 35S::GUS vector (Fig. 10C). This perinuclear distribution is similar to that of other karyopherins (Fornerod et al., 1997; Görlich et al., 1997; Kudo et al., 1997; Rout et al., 1997) and suggests that HST has a role in nucleocytoplasmic transport. The polarized distribution of HST in trichomes is particularly interesting because it suggests that asymmetric nucleocytoplamic transport may contribute to trichome cell polarity.

DISCUSSION

We show that *HST* is the *Arabidopsis* ortholog of *Xpo5* in mammals and *MSN5* in yeast, and describe the phenotype of a loss-of-function mutation in this gene. *HST* is one of at least 17 importin β-like genes in *Arabidopsis*; a similar number exist in yeast and humans (Görlich and Kutay, 1999; Chook and Blobel, 2001). This remarkable conservation of gene number, as well as evidence that at least two members of this family are capable of mediating nucleocytoplasmic transport (Haasen et al., 1999; Jiang et al., 1998b), suggests that the function of these proteins has been largely conserved in plants. Although we have yet to demonstrate that HST regulates nucleocytoplasmic transport, the observation that it interacts with Ran, and its perinuclear distribution, is consistent with this function.

The potential cargo molecules of HST are difficult to predict because its orthologs in yeast and mammals have quite different functions. In yeast, Msn5p exports phosporylated forms of several different transcription factors (Blondel et al., 1999; Boustany and Cyert, 2002; DeVit and Johnston, 1999; Gorner et al., 2002; Kaffman et al., 1998; Komeili et al., 2000) and imports RPA (Yoshida and Blobel, 2001), a protein involved in DNA replication and repair. Loss-of-function mutations in *MSN5* cause defects in the processes in which these factors are involved, demonstrating that Msn5p has an essential function. The function of Xpo5 is more controversial. Brownawell and Macara (Brownawell and Macara, 2002) concluded that Xpo5 is a general exporter of double-stranded RNA-binding proteins (dsRNA-BP) because it binds to and exports the dsRNA-BP interleukin enhancer-binding factor 3 (ILF3), and it interacts in vitro with the dsRNA-binding domains of several other proteins. Other investigators (Bohnsack et al., 2002; Calado et al., 2002) have demonstrated that Xpo5 exports tRNAs and regulates the export of the translation factor eELF1a indirectly, through the association of eELF1a with tRNAs. The interaction between Xpo5 and ILF3 is also regulated by dsRNA (Brownawell and Macara, 2002) but the functional significance of this observation remains unclear. Brownawell and Macara (Brownawell and Macara, 2002) conclude that binding of ILF3 to dsRNA occurs in the cytoplasm and promotes the dissociation of ILF3 from Xpo5, whereas Bohnsack et al. (Bohnsack et al., 2002) propose that the interaction between Xpo5 and ILF3 is actually mediated by dsRNA and is essential for the export of ILF3. These latter investigators propose that Xpo5 primarily regulates RNA export, not protein export. This conclusion is supported by the recent results of Gwizek et al. (Gwizek et al., 2003), which indicate that Xpo5 preferentially exports RNAs that possess a 20-nucleotide minihelix with a base-paired 5′ end and an unpaired 3′ end. These investigators suggest that the primary cargo molecules of

Xpo5 may be siRNAs involved in gene silencing and the double-stranded precursors of miRNAs.

Whatever the cargo molecules of HST may be, the phenotype of *hst-1* suggests that they include factors required for plant growth as well as factors that have more specific regulatory functions. A general requirement for HST is evident in the relatively small size and reduced growth rate of essentially all the organs of mutant plants. HST is also required for the growth and/or organization of the shoot apical meristem (SAM), as demonstrated by the aberrant morphology of the SAM in mutant seedlings and the transient delay in leaf initiation after germination. We tested the sensitivity of *hst-1* seedlings to auxin, cytokinin and abscisic acid but observed no major effect of these hormones on root or hypocotyl growth (M.-Y.P. and R.S.P., unpublished). Thus, the hormonal basis, if any, for this growth defect is unclear. An alternative possibility is that this growth defect results from a change in cell identity. Mutations that disrupt radial patterning in the root, for example, have an effect on root growth similar to that of *hst-1* (Benfey et al., 1993). However, we do not think this explains the effect of *hst-1* on root and hypocotyl elongation because *hst-1* has no major effect on the cellular organization of these structures. We are intrigued by the evidence that Xpo5 exports tRNAs and other double-stranded RNAs because defects in the export of this class of RNAs would be expected to have widespread effects on growth, like those observed in *hst* mutants.

It is unlikely that HST transports only factors with housekeeping functions because of the developmental specificity of many aspects of its mutant phenotype. In a previous study, we showed that *hst-1* accelerated abaxial trichome production and increased the sensitivity of plants to the floral promoter LFY. This leads to the conclusion that HST normally acts to promote the expression of the juvenile phase and/or to repress the expression of the adult phase (Telfer and Poethig, 1998). Because the effect of *hst-1* on abaxial trichome production can also be attributed to a change in leaf polarity, we examined its effects on two non-polarized heteroblastic traits: adaxial trichome density and leaf shape (Fig. 3). We found that *hst-1* accelerates changes in both of these traits, which supports our previous conclusion about its role in phase change. This conclusion is also supported by the fact that the early flowering phenotype of *hst-1* is completely accounted for by its effect on the duration of the juvenile and intermediate phases of shoot development; under CL, it has little or no effect on the duration of the adult phase. This specific effect on the duration of the juvenile phase is unusual. Other flowering time mutations whose effect on vegetative phase change has been studied have either no effect on the duration of the juvenile phase (Martinez-Zapater et al., 1995; Melzer et al., 1999; Scott et al., 1999; Telfer et al., 1997; Weigel and Nilsson, 1995) or affect the duration of both the juvenile and adult phases of development (Gomez-Mena et al., 2001; Soppe et al., 1999; Telfer et al., 1997). *hst-1* is also unusual in that it has a completely opposite effect on flowering time in SD. Under these conditions, mutant plants display accelerated vegetative phase change but are extremely late flowering. One possible interpretation of this phenotype is that HST has different functions in vegetative phase change and floral induction. Early in shoot development, HST promotes the juvenile vegetative phase and reproductive incompetence, whereas during the adult phase it acts to promote flowering under SD but plays no direct role in floral induction under LD. These functions may be carried out by different molecules that require HST for their nucleocytoplasmic transport.

How might HST regulate phase change? Because overexpression of *HST* has no effect on the timing of vegetative phase change or floral induction, it is unlikely that these processes are regulated by a change in the transcription of *HST*. One possibility is that phase change is regulated by post-transcriptional modulation of the amount or activity of HST, as occurs in the case of CRM1 during *Xenopus* embryogenesis (Callanan et al., 2000). A second possibility is that phase change is regulated by a change in the amount or character of the cargo molecules transported by HST, not by changes in the activity of HST itself. In this scenario, HST would have a permissive function, rather than a regulatory one. We favor the latter hypothesis because *hst-1* has a phenotype in every part of the plant, implying that HST is active at all times and in all tissues. However, the possibility that HST is post-transcriptionally regulated in certain tissues cannot be excluded.

Along with promoting the production of trichomes on the abaxial surface of basal leaves in the rosette, *hst-1* reduces the lobing of cells in lower mesophyll layer of the leaf, causes up-rolling of the leaf blade, and produces carpels that are partially unfused and bear ovules on their external (adaxial) margin. *hst-1* also interacts synergistically with *kan* to increase abaxial trichome production and enhances the polarity defects in *kan; pkl* carpels (Eshed et al., 2001). These features are typical of adaxialized mutants (Bowman, 2000; Eshed et al., 2001; Kerstetter et al., 2001; McConnell et al., 2001), and suggest that HST may be required for the specification of abaxial cell identity in both leaves and floral organs. However, whether HST regulates leaf polarity independently of its role in phase change is unclear. Although adaxial-abaxial polarity is an inherent feature of all lateral organs, the way in which this polarity is expressed varies in different organs and at different stages of shoot development. For example, the first two leaves of the rosette are usually flat, subsequent rosette leaves curve downward, inflorescence leaves are flat, and sepals, petals and carpels curve upward (Griffith et al., 1999). Similarly, trichomes are restricted to the adaxial surface of juvenile leaves, are present on both surfaces of adult leaves and are confined to the abaxial surface of leaves in the inflorescence. Many polarized traits in other organisms are also expressed phase specifically (Kerstetter and Poethig, 1998). This phenomenon implies that the mechanism that establishes the adaxial-abaxial polarity of an organ is regulated at some level by the mechanism that specifies the phase identity of the organ. Thus, although it is possible that HST regulates organ polarity independently of its role in phase change, it is also possible that the effect of HST on organ polarity is actually mediated by its effect on phase change.

The basis for the mutant phenotype of *HST* will only become apparent, of course, when its cargo molecules have been identified. This pleiotropic phenotype suggests that HST transports many different molecules, some of which have regulatory functions. We are particularly interested in the possibility that HST regulates the transport of tRNAs and other double-stranded RNAs and their associated proteins. This hypothesis is not only suggested by function of Xpo5, but is also consistent with the observation that mutations in *PAUSED*,

the *Arabidopsis* ortholog of the tRNA export receptor exportin t, are phenotypically similar to *hst* (C.H. and R.S.P., unpublished) (Telfer et al., 1997). Further studies should reveal the types of molecules transported by HST and add to our understanding of the role of nucleocytoplasmic transport in plant growth and development.

We are grateful to the Arabidopsis Biological Resource Center, Joe Ecker (Salk Institute) and Detlef Weigel (Salk Institute) for materials used in this study. Randall Kerstetter provided helpful advice and Hui Sun provided valuable technical assistance. The comments of Jeongsik Yong are also gratefully acknowledged. This work was supported by grants from NIH to K.M.B. and C.H., and by grants from NIH and NSF to R.S.P.

REFERENCES

Alepuz, P. M., Matheos, D., Cunningham, K. W. and Estruch, F. (1999). The *Saccharomyces cerevisiae* RanGTP-binding protein Msn5p is involved in different signal transduction pathways. *Genetics* **153**, 1219-1231.

Andrade, M. A., Petosa, C., O'Donoghue, S. I., Muller, C. W. and Bork, P. (2001). Comparison of ARM and HEAT protein repeats. *J. Mol. Biol.* **309**, 1-18.

Ballas, N. and Citovsky, V. (1997). Nuclear localization signal binding protein from Arabidopsis mediates nuclear import of Agrobacterium VirD2 protein. *Proc. Natl. Acad. Sci. USA* **94**, 10723-10728.

Bancroft, I. and Dean, C. (1993). Transposition pattern of the maize element Ds in *Arabidopsis thaliana*. *Genetics* **134**, 1221-1229.

Benfey, P. N., Linstead, P. J., Roberts, K., Schiefelbein, J. W., Hauser, M. T. and Aeschbacher, R. A. (1993). Root development in *Arabidopsis*: four mutants with dramatically altered root morphogenesis. *Development* **119**, 57-70.

Berardini, T. Z., Bollman, K., Sun, H. and Poethig, R. S. (2001). Regulation of vegetative phase change in *Arabidopsis thaliana* by cyclophilin 40. *Science* **291**, 2405-2407.

Berna, G., Robles, P. and Micol, J. L. (1999). A mutational analysis of leaf morphogenesis in *Arabidopsis thaliana*. *Genetics* **152**, 729-742.

Blazquez, M. A., Soowal, L. N., Lee, I. and Weigel, D. (1997). *LEAFY* expression and flower initiation in *Arabidopsis*. *Development* **124**, 3835-3844.

Blondel, M., Alepuz, P. M., Huang, L. S., Shaham, S., Ammerer, G. and Peter, M. (1999). Nuclear export of Far1p in response to pheromones requires the export receptor Msn5p/Ste21p. *Genes Dev.* **13**, 2284-2300.

Bohnsack, M. T., Regener, K., Schwappach, B., Saffrich, R., Paraskeva, E., Hartmann, E. and Görlich, D. (2002). Exp5 exports eEF1A via tRNA from nuclei and synergises with other transport pathways to confine translation to the cytoplasm. *EMBO J.* **21**, 6205-6215.

Boustany, L. M. and Cyert, M. S. (2002). Calcineurin-dependent regulation of Crz1p nuclear export requires Msn5p and a conserved calcineurin docking site. *Genes Dev.* **16**, 608-619.

Bowman, J. L. (2000). The *YABBY* gene family and abaxial cell fate. *Curr. Opin. Plant Biol.* **3**, 17-22.

Brownawell, A. M. and Macara, I. G. (2002). Exportin-5, a novel karyopherin, mediates nuclear export of double-stranded RNA binding proteins. *J. Cell Biol.* **156**, 53-64.

Calado, A., Treichel, N., Muller, E.-C., Otto, A. and Kutay, U. (2002). Exportin-5-mediated nuclear export of eukaryotic elongation factor 1A and tRNA. *EMBO J.* **21**, 6216-6224.

Callanan, M., Kudo, N., Gout, S., Brocard, M., Yoshida, M., Dimitrov, S. and Khochbin, S. (2000). Developmentally regulated activity of CRM1/XPO1 during early Xenopus embryogenesis. *J. Cell Sci.* **113**, 451-459.

Chien, J. C. and Sussex, I. M. (1996). Differential regulation of trichome formation on the adaxial and abaxial leaf surfaces by gibberellins and photoperiod in *Arabidopsis thaliana* (L) Heynh. *Plant Physiol.* **111**, 1321-1328.

Chook, Y. M. and Blobel, G. (2001). Karyopherins and nuclear import. *Curr. Opin. Struct. Biol.* **11**, 703-715.

Clough, S. J. and Bent, A. F. (1998). Floral dip: a simplified method for Agrobacterium-mediated transformation of Arabidopsis thaliana. *Plant J.* **16**, 735-743.

DeVit, M. J. and Johnston, M. (1999). The nuclear exportin Msn5 is required for nuclear export of the Mig1 glucose repressor of Saccharomyces cerevisiae. *Curr. Biol.* **9**, 1231-1241.

Eshed, Y., Baum, S. F., Perea, J. V. and Bowman, J. L. (2001). Establishment of polarity in lateral organs of plants. *Curr. Biol.* **11**, 1251-1260.

Fornerod, M., van Deursen, J., van Baal, S., Reynolds, A., Davis, D., Murti, K. G., Fransen, J. and Grosveld, G. (1997). The human homologue of yeast CRM1 is in a dynamic subcomplex with CAN/Nup214 and a novel nuclear pore component Nup88. *EMBO J.* **16**, 807-816.

Gomez-Mena, C., Pineiro, M., Franco-Zorrilla, J. M., Salinas, J., Coupland, G. and Martinez-Zapater, J. M. (2001). *early bolting in short days*: an Arabidopsis mutation that causes early flowering and partially suppresses the floral phenotype of *leafy*. *Plant Cell* **13**, 1011-1024.

Görlich, D., Dabrowski, M., Bischoff, F. R., Kutay, U., Bork, P., Hartmann, E., Prehn, S. and Izaurralde, E. (1997). A novel class of RanGTP binding proteins. *J. Cell Biol.* **138**, 65-80.

Görlich, D. and Kutay, U. (1999). Transport between the cell nucleus and the cytoplasm. *Annu. Rev. Cell Dev. Biol.* **15**, 607-660.

Gorner, W., Durchschlag, E., Wolf, J., Brown, E. L., Ammerer, G., Ruis, H. and Schuller, C. (2002). Acute glucose starvation activates the nuclear localization signal of a stress-specific yeast transcription factor. *EMBO J.* **21**, 135-144.

Griffith, M. E., da Silva Conceicao, A. and Smyth, D. R. (1999). *PETAL LOSS* gene regulates initiation and orientation of second whorl organs in the *Arabidopsis* flower. *Development* **126**, 5635-5644.

Gwizdek, C., Ossareh-Nazari, B., Brownawell, A. M., Doglio, A., Betrand, E., Macara, I. G. and Dargemont, C. (2003). Exportin-5 mediates nuclear export of minihelix-containing RNAs. *J. Biol. Chem.* (in press).

Haasen, D., Kohler, C., Neuhaus, G. and Merkle, T. (1999). Nuclear export of proteins in plants: AtXPO1 is the export receptor for leucine-rich nuclear export signals in Arabidopsis thaliana. *Plant J.* **20**, 695-705.

Haizel, T., Merkle, T., Pay, A., Fejes, E. and Nagy, F. (1997). Characterization of proteins that interact with the GTP-bound form of the regulatory GTPase Ran in Arabidopsis. *Plant J.* **11**, 93-103.

Hicks, G. R. and Raikhel, N. V. (1995). Protein import into the nucleus: an integrated view. *Annu. Rev. Cell Dev. Biol.* **11**, 155-188.

Hubner, S., Smith, H. M., Hu, W., Chan, C. K., Rihs, H. P., Paschal, B. M., Raikhel, N. V. and Jans, D. A. (1999). Plant importin alpha binds nuclear localization sequences with high affinity and can mediate nuclear import independent of importin beta. *J. Biol. Chem.* **274**, 22610-22617.

Jensen, W. A. (1962). *Botanical Histochemistry*. San Francisco: W. H. Freeman.

Jiang, C. J., Imamoto, N., Matsuki, R., Yoneda, Y. and Yamamoto, N. (1998a). Functional characterization of a plant importin alpha homologue. Nuclear localization signal (NLS)-selective binding and mediation of nuclear import of nls proteins in vitro. *J. Biol. Chem.* **273**, 24083-24087.

Jiang, C. J., Imamoto, N., Matsuki, R., Yoneda, Y. and Yamamoto, N. (1998b). In vitro characterization of rice importin beta1: molecular interaction with nuclear transport factors and mediation of nuclear protein import. *FEBS Lett.* **437**, 127-130.

Jiang, C. J., Shoji, K., Matsuki, R., Baba, A., Inagaki, N., Ban, H., Iwasaki, T., Imamoto, N., Yoneda, Y., Deng, X. W. et al. (2001). Molecular cloning of a novel importin alpha homologue from rice, by which constitutive photomorphogenic 1 (COP1) nuclear localization signal (NLS)-protein is preferentially nuclear imported. *J. Biol. Chem.* **276**, 9322-9329.

Kaffman, A. and O'Shea, E. K. (1999). Regulation of nuclear localization: a key to a door. *Annu. Rev. Cell Dev. Biol.* **15**, 291-339.

Kaffman, A., Rank, N. M., O'Neill, E. M., Huang, L. S. and O'Shea, E. K. (1998). The receptor Msn5 exports the phosphorylated transcription factor Pho4 out of the nucleus. *Nature* **396**, 482-486.

Kerstetter, R. A. and Poethig, R. S. (1998). The specification of leaf identity during shoot development. *Annu. Rev. Cell Dev. Biol.* **141**, 373-398.

Kerstetter, R. A., Bollman, K., Taylor, R. A., Bomblies, K. and Poethig, R. S. (2001). *KANADI* regulates organ polarity in Arabidopsis. *Nature* **411**, 706-709.

Kieber, J. J., Rothenberg, M., Roman, G., Feldmann, K. A. and Ecker, J. R. (1993). *CTR1*, a negative regulator of the ethylene response pathway in Arabidopsis, encodes a member of the raf family of protein kinases. *Cell* **72**, 427-441.

Kim, S. H., Arnold, D., Lloyd, A. and Roux, S. J. (2001). Antisense expression of an Arabidopsis ran binding protein renders transgenic roots

hypersensitive to auxin and alters auxin-induced root growth and development by arresting mitotic progress. *Plant Cell* **13**, 2619-2630.

Komeili, A. and O'Shea, E. K. (2001). New perspectives on nuclear transport. *Annu. Rev. Genet.* **35**, 341-364.

Komeili, A., Wedaman, K. P., O'Shea, E. K. and Powers, T. (2000). Mechanism of metabolic control. Target of rapamycin signaling links nitrogen quality to the activity of the Rtg1 and Rtg3 transcription factors. *J. Cell Biol.* **151**, 863-878.

Kudo, N., Khochbin, S., Nishi, K., Kitano, K., Yanagida, M., Yoshida, M. and Horinouchi, S. (1997). Molecular cloning and cell cycle-dependent expression of mammalian CRM1, a protein involved in nuclear export of proteins. *J. Biol. Chem.* **272**, 29742-29751.

Lippai, M., Tirian, L., Boros, I., Mihaly, J., Erdelyi, M., Belecz, I., Mathe, E., Posfai, J., Nagy, A., Udvardy, A. et al. (2000). The *Ketel* gene encodes a Drosophila homologue of importin-beta. *Genetics* **156**, 1889-1900.

Lorenzen, J. A., Baker, S. E., Denhez, F., Melnick, M. B., Brower, D. L. and Perkins, L. A. (2001). Nuclear import of activated D-ERK by DIM-7, an importin family member encoded by the gene *moleskin*. *Development* **128**, 1403-1414.

Macara, I. G. (2001). Transport into and out of the nucleus. *Microbiol. Mol. Biol. Rev.* **65**, 570-594.

Martinez-Zapater, J. M., Jarillo, J., Cruz-Alvarez, M., Roldan, M. and Salinas, J. (1995). *Arabidopsis* late-flowering *fve* mutants are affected in both vegetative and reproductive development. *Plant J.* **7**, 543-551.

McConnell, J. R., Emery, J., Eshed, Y., Bao, N., Bowman, J. and Barton, M. K. (2001). Role of *PHABULOSA* and *PHAVOLUTA* in determining radial patterning in shoots. *Nature* **411**, 709-713.

Melzer, S., Kampmann, G., Chandler, J. and Apel, K. (1999). *FPF1* modulates the competence to flowering in Arabidopsis. *Plant J.* **18**, 395-405.

Merkle, T. (2001). Nuclear import and export of proteins in plants: a tool for the regulation of signaling. *Planta* **213**, 499-517.

Nakielny, S. and Dreyfuss, G. (1999). Transport of proteins and RNAs in and out of the nucleus. *Cell* **99**, 677-690.

Röbbelen, G. (1957). Über Heterophyllie bei *Arabidopsis thaliana* (L.) Heynh. *Ber. Dtsch. Bot. Ges.* **70**, 39-44.

Rose, A. and Meier, I. (2001). A domain unique to plant RanGAP is responsible for its targeting to the plant nuclear rim. *Proc. Natl. Acad. Sci. USA* **98**, 15377-15382.

Rout, M. P., Blobel, G. and Aitchison, J. D. (1997). A distinct nuclear import pathway used by ribosomal proteins. *Cell* **89**, 715-725.

Sambrook, J., Fritsch, E. F. and Maniatis, T. (1989). *Molecular Cloning.* Cold Spring Harbor, NY: Cold Spring Harbor Laboratory Press.

Scott, D. B., Jin, W., Ledford, H. K., Jung, H. S. and Honma, M. A. (1999). *EAF1* regulates vegetative-phase change and flowering time in Arabidopsis. *Plant Physiol.* **120**, 675-684.

Serrano-Cartagena, J., Candela, H., Robles, P., Ponce, M. R., Perez-Perez, J. M., Piqueras, P. and Micol, J. L. (2000). Genetic analysis of *incurvata* mutants reveals three independent genetic operations at work in Arabidopsis leaf morphogenesis. *Genetics* **156**, 1363-1377.

Siegfried, K. R., Eshed, Y., Baum, S. F., Otsuga, D., Drews, G. N. and Bowman, J. L. (1999). Members of the *YABBY* gene family specify abaxial cell fate in Arabidopsis. *Development* **126**, 4117-4128.

Smith, H. M. and Raikhel, N. V. (1999). Protein targeting to the nuclear pore. What can we learn from plants? *Plant Physiol.* **119**, 1157-1164.

Smith, H. M., Hicks, G. R. and Raikhel, N. V. (1997a). Importin alpha from *Arabidopsis thaliana* is a nuclear import receptor that recognizes three classes of import signals. *Plant Physiol.* **114**, 411-417.

Smith, H. M. S., Hicks, G. R. and Raikhel, N. V. (1997b). Importin alpha from *Arabidopsis thaliana* is a nuclear import receptor that recognizes three classes of import signals. *Plant Physiol.* **114**, 411-417.

Soppe, W. J., Bentsink, L. and Koornneef, M. (1999). The early-flowering mutant *efs* is involved in the autonomous promotion pathway of *Arabidopsis thaliana*. *Development* **126**, 4763-4770.

Steynen, Q. J., Bolokoski, D. A. and Schultz, E. A. (2001). Alteration in flowering time causes accelerated or decelerated progression through Arabidopsis vegetative phases. *Can. J. Bot.* **79**, 657-665.

Tekotte, H., Berdnik, D., Torok, T., Buszczak, M., Jones, L. M., Cooley, L., Knoblich, J. A. and Davis, I. (2002). *Dcas* Is Required for importin-alpha3 nuclear export and mechano-sensory organ cell fate specification in Drosophila. *Dev. Biol.* **244**, 396-406.

Telfer, A. and Poethig, R. S. (1994). Leaf development in Arabidopsis. In *Arabidopsis* (ed. E. M. Meyerowitz and C. R. Somerville), pp. 379-401. Cold Spring Harbor, NY: Cold Spring Harbor Press.

Telfer, A. and Poethig, R. S. (1998). *HASTY*: a gene that regulates the timing of shoot maturation in *Arabidopsis thaliana*. *Development* **125**, 1889-1898.

Telfer, A., Bollman, K. M. and Poethig, R. S. (1997). Phase change and the regulation of trichome distribution in *Arabidopsis thaliana*. *Development* **124**, 645-654.

Tirian, L., Puro, J., Erdelyi, M., Boros, I., Papp, B., Lippai, M. and Szabad, J. (2000). The *Ketel(D)* dominant-negative mutations identify maternal function of the Drosophila importin-beta gene required for cleavage nuclei formation. *Genetics* **156**, 1901-1912.

Tsukaya, H., Shoda, K., Kim, G. T. and Uchimiya, H. (2000). Heteroblasty in *Arabidopsis thaliana* (L.) Heynh. *Planta* **210**, 536-542.

Ward, B. M. and Lazarowitz, S. G. (1999). Nuclear export in plants. Use of geminivirus movement proteins for a cell-based export assay. *Plant Cell* **11**, 1267-1276.

Weigel, D. and Nilsson, O. (1995). A developmental switch sufficient for flower initiation in diverse plants. *Nature* **377**, 495-500.

Yoshida, K. and Blobel, G. (2001). The karyopherin Kap142p/Msn5p mediates nuclear import and nuclear export of different cargo proteins. *J. Cell Biol.* **152**, 729-740.